Error Correction Method for Rotating Axis of Large Rotating Machinery Based on Machine Vision

Yu-Shuo Tan[1(✉)], Wen-Bin Zhang[2], Jing Wang[3], Han Han[1], and Wei-Ping Cao[4]

[1] Shijiazhuang Posts and Telecommunications Technical College, Shijiazhuang 050021, Hebei, China
ls62322@aliyun.com
[2] Honghe University, Mengzi 661199, China
[3] Shijiazhuang Information Engineering Vocational College, Shijiazhuang 050000, China
[4] West Normal University Physical Culture Institute Chengdu, Nanchong 637099, Sichuan, China

Abstract. The error model of the traditional error correction method has data deviation, which leads to a decline in the ability to identify and separate error data during the error correction process. For this reason, this research proposes a new method of error correction for the rotating shaft of large rotating machinery based on machine vision technology. This method redesigns the shaft error check code and optimizes the shaft error model of large rotating machinery. Then based on the machine vision to detect the shaft error, and realize the reliable correction of the shaft error. The experimental results show that: compared with the traditional method, the recognition similarity coefficient of this method is closer to 1, and the error data separation effect is also superior to the traditional method.

Keywords: Machine vision · Mechanical axis of rotation · Error correction · Error check code

1 Introduction

In the working process of rotating shaft of large rotating machinery, due to the technical errors of manufacturing technology and production process, the rotating effect of rotating shaft may be affected. When this kind of situation occurs, if the detailed and accurate error correction is not carried out, the work efficiency of large rotating machinery will be affected. Therefore, it is one of the effective measures to design an effective error correction method for large rotating machinery to ensure the work efficiency and use safety of large rotating machinery.

Machine vision, also known as computer vision, refers to data measurement and discrimination by machine instead of human eyes. Through the use of machine vision technology, the ability to detect the error data is strengthened, the accuracy of the detection results is improved, and the advanced technical support is provided for the normal operation of the national large-scale rotating machinery.

W. Fu et al. (Eds.): ICMTEL 2021, LNICST 387, pp. 39–50, 2021.
https://doi.org/10.1007/978-3-030-82562-1_4

For this reason, this paper proposes a method of error correction for large rotating machinery based on machine vision. This method redesigns the shaft error check code and optimizes the shaft error model of large rotating machinery. Then, the rotation axis error is detected based on machine vision to realize the reliable correction of the rotation axis error.

2 Error Correction Method for Rotating Shaft of Large Rotating Machinery

2.1 Design Shaft Error Check Code

In the initial stage of error correction of the rotating shaft of large rotating machinery, the shaft error check code is compiled in advance. The design requires that the check code has a shortened basic structure feature, and the check code is used to detect large-scale rotating machinery and basic rotation axis data to obtain the error information flow existing therein. The basic structure of the designed check code is shown in Fig. 1 below.

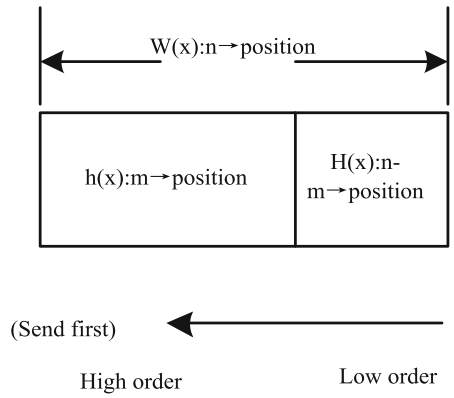

Fig. 1. Basic structure of cyclic redundancy check code

According to the label in Fig. 1, it can be seen that there is a one-to-one correspondence between the m coefficients of $h(x)$ and the m information bits; the $n - m$ coefficients of $H(x)$ correspond to the $n - m$ check bits. From the perspective of channel coding, the entire n bit frame is a codeword, so the $n - m$ parity part is used as the designed check code. Among them, $h(x)$ is a polynomial of degree $(m - 1)$, $H(x)$ is a polynomial of degree $(n - m - 1)$, then $W(X)$ is a polynomial of degree $(m - 1)$, and $k(x)$ is a polynomial of degree $(n - m)$ [1, 2]. Therefore, the cyclic code has a formula at the sending end:

$$W(X) = x^{n-m}h(x) + H(x) \tag{1}$$

In formula (1): $W(X)$ represents the transmission code; $H(x) = \frac{x^{n-m}h(x)}{k(x)}$. If there is no error code in the received code stream, then the received code $H(x)$ should be equal

to the transmit code $W(X)$, that is, there is:

$$W(X) = H(x) = x^{n-m}h(x) + H(x) = \varphi(x)k(x) \tag{2}$$

The received code $H(x)$ at this time can be divisible by the generator polynomial $k(x)$. If the received code at this time cannot be divisible by $k(x)$, it means that a code error occurred during the transmission of the shaft data. At this time, the "cyclic" feature of the check code is shown in the cyclic code generator polynomial $k(x)$, and the length of the check bit is $n - m$, which is the embodiment of "redundancy" [3]. Because this code is a cyclic code, it exists:

$$k(x)\mu(x) = x^2 + 1 \tag{3}$$

Here $n - m$ is a factor of n. If $n - m$ is fixed, then parameter n is also fixed. However, in the actual check, the frame length n can be changed continuously, so the cyclic code (n_0, m_0) is shortened to any s bit, and the actual check code is obtained as follows:

$$(n_0 - s, m_0 - s) = (n, m) \tag{4}$$

The shortened check code still has inherent characteristics. Through the analysis and control of the cyclic code, it can be applied to the basic check of the error of the rotating shaft of large rotating machinery [4].

2.2 Setting up Error Model of Rotating Axis of Large Rotating Machinery

Because large-scale rotating machinery is prone to abnormal system operation during the control process, coupled with the influence of basic control hardware and matching errors, it is necessary to establish a rotating axis error model based on the basic structure of large-scale rotating machinery, and meet machine vision inspection according to this model The basic application conditions to obtain the rotation error data.

Suppose the ideal point control position of the rotating shaft of a large rotating machine is $b_1(x_i, y_i)$, and the error point position coordinate is $b_2(x_j, y_j)$, where x_i and x_j represent the abscissa of the point; y_i and y_j represent the ordinate of the point [5]. The relationship between the two points can be expressed by the following formula:

$$\begin{bmatrix} x_a \\ y_a \end{bmatrix} = \left(1 + q_1 d^2 + q_2 d^4\right)\begin{bmatrix} x' \\ y' \end{bmatrix} + \begin{bmatrix} 2\gamma_1 x'y' + \gamma_2\left(d^2 + 2x^2\right) \\ \gamma_1\left(d^2 + 2y^2\right) + 2\gamma_2 x'y' \end{bmatrix} \tag{5}$$

In formula (5): $x' = \frac{x_n - x_{n0}}{\mu_{nx}}$, $y' = \frac{y_n - y_{n0}}{\mu_{ny}}$; where x_{n0} and y_{n0} represent the initial data position coordinates of the ideal point; μ_{nx} and μ_{ny} respectively represent the separation functions of the ideal point coordinates. $d = x'^2 + y'^2$. x' and y' represent the median value of ideal point and error point respectively. $x_a = \frac{x_m - x_{m0}}{\mu_{mx}}$, $y_a = \frac{y_m - y_{m0}}{\mu_{my}}$. Where x_{m0} and y_{m0} are the initial coordinates of the error points; μ_{mx} and μ_{my} are the separation functions of the coordinates of the error points. x_a. y_a is the coordinate value when the correlation strength is a; q_1 and q_2 are the radial error coefficients of the error points; γ_1

and γ_2 are the tangential error coefficients. Due to the error in the relationship processing, an objective function is set up to optimize the influence parameters in the relationship value

$$r = \min\left(\sum_{i=1}^{n}\sum_{j=1}^{m}\left\|\eta_{nij} - \eta\left(A_n, C, Q_i, \eta_{tj}\right)\right\|^2\right) \tag{6}$$

In formula (6): r represents the objective function; η_{nij} represents the plane coordinates of the j marking point in the i measurement area in the ideal point coordinates; A_n represents the mechanical internal parameter matrix; C represents the degree of error index; Q_i represents the i The external parameter matrix in each area; η_{tj} represents the point function of t at the measurement time. Combining formulas (5) and (6) to set the shaft error model as:

$$\begin{matrix} b_1 \\ b_2 \end{matrix} T = r(x_a, y_a) \tag{7}$$

In formula (7): $\begin{matrix} b_1 \\ b_2 \end{matrix} T$ represents the error model under the influence of ideal point and error point [6].

According to the above design, the error parameters of the rotating shaft of large rotating machinery are screened to realize the error detection of machine vision.

2.3 Detection of Shaft Error Based on Machine Vision

The above model is used to obtain the rotation axis error detection feature. According to this feature, the machine vision reverse perception algorithm is used to detect the error. The main detection device is a multilayer perceptron. Using machine vision detection algorithm, the working signal of the rotating shaft is forward divergent and propagated, and the expected value is established. When the signal does not reach the expected value, the signal is defined as an error signal, and the signal is propagated back. Start at the output of the device and spread down layer by layer. Select the initial measurement value of the coefficient, make the sample data input into the sensor $u = (u_0, u_1, \ldots, u_{n-1})$, detect the expected output value of $v = (v_0, v_1, \ldots, v_{n-1})$, and the actual output value of $z = (z_0, z_1, \ldots, z_{n-1})$, adjust the coefficient gradually downward from the layer area where the output terminal is located, and get the adjustment The result is:

$$\phi_{mn}(t+1) = \phi_{mn}(t) + \beta\lambda_n \cdot \delta_m \tag{8}$$

In formula (8): m and n are input layer nodes, ϕ_{mn} is coefficient weight between input layer node m and node n in t period; β is gain term; λ_n is deviation at node$n$; δ_m is data feature of m node [7]. When n is the output layer node by default, then:

$$\lambda_n = z_n \cdot (1 - z_n) \cdot (v_n - z_n) \tag{9}$$

In formula (9): v_n is the expected output value of node n; z_n is the actual output of node$n$. When there is a hidden middle layer in the n node, then:

$$\lambda_n = \varepsilon_n\left(1 - \varepsilon'_{\boldsymbol{n}}\right)\sum_{i=1}^{n}\lambda_u \cdot \alpha_{nu} \tag{10}$$

In formula (10): u represents the number of nodes in the upper layer of node$n$; α_{nu} represents the coefficient convergence parameter under these two nodes. According to the obtained λ_n, the error type of rotation axis is determined, so as to realize the error detection based on machine vision [8].

2.4 Error Correction

Based on the above processing, the error correction process of rotating axis can be deduced as follows:

$$F = G^2\lambda^3 + E_{count} \tag{11}$$

In formula (11): G represents the coefficient matrix; λ represents the error of the measurement point; E_{count} represents the constant term [9]. Continuously transform the error coefficient λ of the above formula, calculate the values of different correction coefficients λ, and obtain the correction model coefficients according to the relationship between the two values, as shown in Table 1:

Table 1. Correction model coefficients

	F1	F2	F3
ε1	0.344	− 0.128	0.103
ε2	0.251	− 0.07	0.055
ε3	0.035	− 0.029	0.266
ε4	− 0.191	0.248	− 0.047
ε5	− 0.032	0.066	0.401
ε6	0.076	− 0.738	− 0.189
ε7	− 0.029	0.107	0.019
ε8	− 0.015	0.219	− 0.304
ε9	− 0.012	− 0.247	− 0.205
ε10	0.026	0.005	0.033
ε11	0.087	− 0.463	0.026
ε12	− 0.266	0.575	− 0.067
ε13	0.645	− 0.372	0.214
ε14	− 0.343	0.641	− 0.035
ε15	− 0.047	0.248	− 0.081

Deal with the coefficients shown in the table above. When the amplitude error exists in the measurement result, calculate the error vector o_r of this part. The calculation formula is as follows:

$$o_r(\lambda, E) = Ga(\lambda, E) \tag{12}$$

In formula (12): G represents the amplitude error matrix, which satisfies the following quantitative relationship:

$$G = diag([c_1, c_2, ..., c_n]^k) \tag{13}$$

In formula (13): c_n is the amplitude coefficient; when c_1 is 1, the amplitude error square wave is (λ_0, E_0), and the corresponding correction array covariance matrix can be expressed as:

$$R = GR_iG^H + \zeta_{\max}c_n \tag{14}$$

In formula (14): G^H represents the magnitude error matrix coefficient; $\zeta_{\max}$ represents the corresponding eigenvector; R_i represents the subspace coefficient. Calculate the value of the corresponding eigenvector in the above formula and use this value as the correction amount. The calculation formula is:

$$\zeta_{\max} = \frac{G(\varepsilon_0, \eta_0)}{\left|G^H\right|^2} \tag{15}$$

According to the actual work of large-scale rotating machinery, considering the particularity of rotating shaft error, the coefficient in the correction process is constantly changed, and the processing process of the above calculation formula is repeated to obtain the position error correction amount of different rotating axes. So far, with the help of machine vision, the error correction of large-scale rotating machinery's rotating axis is realized [10].

3 Experimental Study

In order to verify the effectiveness of the error correction method of large rotating machinery based on machine vision, this method is compared with two traditional correction methods, and the following experiments are designed. Among them, this method is the experimental group, and two traditional correction methods are control group A and control group B. The experiment takes the error data recognition effect, the signal waveform similarity coefficient of the recognition result and the error data separation effect as the indicators to verify the application performance of different methods.

3.1 Error Data Recognition Test

Based on MATLAB to build an experimental platform, the three test groups used different techniques to identify the rotation errors of large rotating machinery before the calibration started. The results are shown in Fig. 2.

Based on this, according to the similarity evaluation function, the data recognition effect of the three test groups is evaluated. It is known that the data signal will form irregular waveforms under different commands. At the same time, the test environment itself will also bring interference to the experimental results, and the identification waveforms often have timing differences. Therefore, according to the correlation, the signal waveforms of the two test groups are judged to be similar to the real signals. The experiment

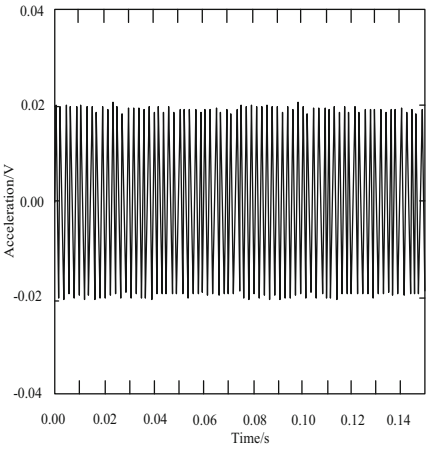

(a) Test results of experimental group

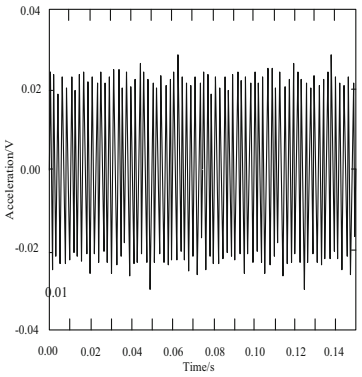

(b) Control group a test results

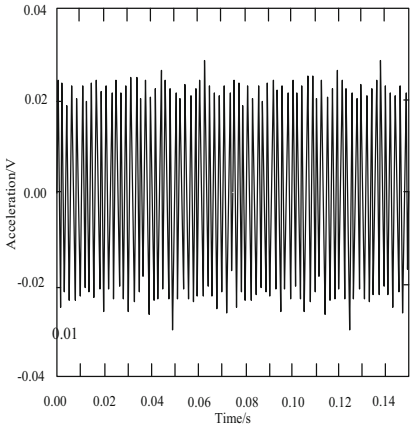

(c) Control group B test results

Fig. 2. Comparison of error data recognition effect

assumes that the real signal and the identification signal are $x(t)$ and $y(t)$ respectively, and the similarity between the waveforms is measured by the error energy. The error energy is expressed as:

$$\int (x(t) - \omega \cdot y(t))^2 dt \tag{16}$$

In formula (16): ω is the multiple value that makes $\omega \cdot y(t)$ close to $x(t)$. At the same time, it is required to ensure that the error of energy can be minimized when the parameter D is selected:

$$\omega = \frac{\int x(t) \cdot y(t) dt}{\int y(t) \cdot y(t) dt} \tag{17}$$

When the above conditions are met, the error energy is known to be the minimum. Therefore, the correlation coefficient between the real signal and the identification signal is defined as σ_{xy}, and the value of the correlation coefficient can be obtained:

$$\sigma_{xy} = \frac{\int x(t) \cdot y(t) dt}{\sqrt{\int x^2(t) dt \cdot y^2(t) dt}} \tag{18}$$

The result σ_{xy} can be used to describe the waveform similarity between the real signal and the recognition signal. In the process of experimental test, there is a time difference ΔT between the real signal and the recognition signal, so the correlation coefficient of the two signals in ΔT time is obtained by multiplication and integration. When the similarity coefficient is 1, the error energy is 0, which indicates that the correction method has the best recognition effect for the error data; when the similarity coefficient is 0, the result of the correction method is the worst. In 40 tests, the statistical results of error signal waveform similarity coefficient of three test groups are shown in Table 2.

Table 2. Test results of signal waveform similarity coefficient

Test group	Experience group	Control group A	Control group B
Group 1	0.9355	0.8574	0.8781
Group 2	0.9346	0.8585	0.8761
Group 3	0.9351	0.8588	0.8763
Group 4	0.9350	0.8573	0.8777
Group 5	0.9348	0.8575	0.8773
Group 6	0.9346	0.8580	0.8766
Group 7	0.9352	0.8581	0.8771
Group 8	0.9345	0.8575	0.8770
Group 9	0.9347	0.8575	0.8772

(*continued*)

Table 2. (*continued*)

Test group	Experience group	Control group A	Control group B
Group 10	0.9351	0.8586	0.8765
Group 11	0.9354	0.8577	0.8780
Group 12	0.9347	0.8584	0.8761
Group 13	0.9352	0.8587	0.8760
Group 14	0.9351	0.8577	0.8775
Group 15	0.9345	0.8576	0.8775
Group 16	0.9347	0.8581	0.8767
Group 17	0.9351	0.8581	0.8771
Group 18	0.9348	0.8577	0.8772
Group 19	0.9348	0.8578	0.8777
Group 20	0.9352	0.8589	0.8764
Group 21	0.9355	0.8575	0.8784
Group 22	0.9347	0.8583	0.8768
Group 23	0.9353	0.8585	0.8769
Group 24	0.9350	0.8577	0.8772
Group 25	0.9349	0.8579	0.8771
Group 26	0.9345	0.8582	0.8769
Group 27	0.9352	0.8586	0.8772
Group 28	0.9349	0.8574	0.8774
Group 29	0.9348	0.8577	0.8777
Group 30	0.9351	0.8585	0.8767
Group 31	0.9350	0.8580	0.8771
Group 32	0.9352	0.8742	0.8599
Group 33	0.9350	0.8765	0.8542
Group 34	0.9345	0.8772	0.8540
Group 35	0.9346	0.8763	0.8432
Group 36	0.9352	0.8769	0.8575
Group 37	0.9328	0.8760	0.8543
Group 38	0.9366	0.8785	0.8519
Group 39	0.9347	0.8799	0.8722
Group 40	0.9387	0.8751	0.8658

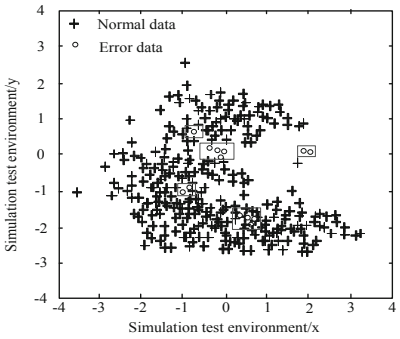

(a) Test results of experimental group

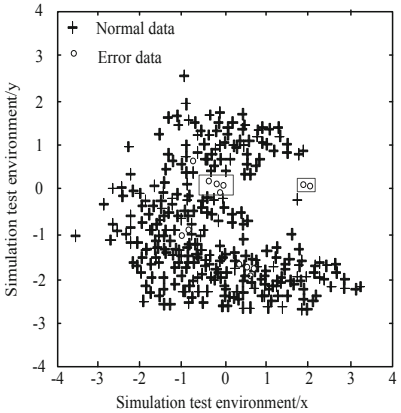

(b) Test results of control group A

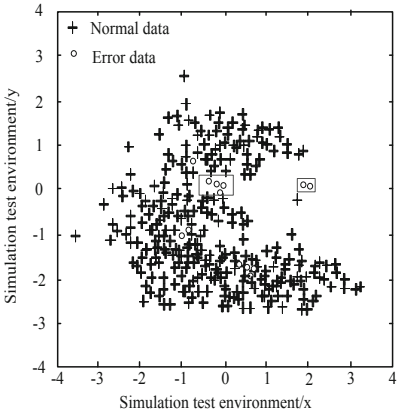

(c) Control group B test results

Fig. 3. Comparison of error data analysis results

According to the 40 test results in Table 2, when the error signal is identified by the method in this paper, there is a higher similarity coefficient between the signal waveform and the real signal waveform, and the similarity coefficient value is closer to 1. It can be seen that compared with the control group, this article has a better recognition effect.

3.2 Error Data Separation Effect Test

Three groups of correction methods are loaded into the same test platform respectively, and the detection effect of different correction methods on error data is compared. The simulation test results are shown in Fig. 3.

According to the test results in Fig. 3, the correction method in the experimental group completely separates the rotation error of large rotating machinery from the normal data. However, due to the lack of machine vision, the correction methods of the two control groups failed to completely separate the error data from the normal data, resulting in the error data separation effect can not reach the expected effect. This shows that the error correction method of large rotating machinery based on machine vision designed in this paper can more accurately separate the error data of large rotating machinery, and can lay an effective foundation for error correction.

4 Concluding Remarks

In this study, a method of large rotating machinery rotation axis error correction based on machine vision is designed. Based on the existing research, the technology function of machine vision is fully used to enhance the recognition and separation of large rotating machinery rotation axis error data, so as to effectively improve the correction effect of large rotating machinery rotation axis error. However, due to the difficulty of this method, we should pay attention to the accuracy of the data in the calculation process to ensure that the correction effect is not disturbed by the conventional calculation.

Acknowledgments. Research on Governance of Elderly Sports Health Promotion Sichuan Education Development Research Center CJF20035.

References

1. Shiguang, L.: Glass-bottle defect detection method based on machine vision. Packag. Eng. **39**(03), 183–187 (2018)
2. Erlin, T., Zuhe, L.: Research on position correction method of picking robot—based on wireless sensor network and ultra wide band FM method. J. Agric. Mech. Res. **41**(02), 216–219+224 (2019)
3. Lin, G., Bo, W.: Vision target calibration and error correction simulation at crossroads. Comput. Simul. **35**(11), 141–144+174 (2018)
4. Tao, L., Shibin, Y., Yongjie, R., et al.: Automatic calibration of robot tool center frame robot tool center frames. Opt. Precis. Eng. **27**(03), 661–670 (2019)
5. Bin, L., Guobin, C., Delian, Z.: Fixing error calibration of inertial measurement system in robot. Coal Mine Mach. **39**(01), 41–44 (2018)

6. Li, Z., Zikai, Z., Xiaodong, X.: Research on attitude angle error correction method of inertial gyroscope. Coal Mine Mach. **39**(06), 50–52 (2018)
7. Shuai, L., Dongye, L., Gautam, S., et al.: Overview and methods of correlation filter algorithms in object tracking. Complex Intell. Syst. (3) 2020 https://doi.org/10.1007/s40747-020-00161-4
8. Liu, S., Li, Z., Zhang, Y., Cheng, X.: Introduction of key problems in long-distance learning and training. Mobile Netw. Appl. **24**(1), 1–4 (2019)
9. Shuai, L., Weiling, B., Nianyin, Z., et al.: A fast fractal based compression for MRI images. IEEE Access **7**, 62412–62420 (2019)
10. Feifei, S., Hong, Z., Kaiyu, Z., et al.: Hysteresis prediction and error correction of GMM current transformer. Electr. Mach. Control **22**(07), 85–90 (2018)